Equivalent dynamic model of DEMES rotary joint

2016 Smart Mater. Struct. 25 075025

(http://iopscience.iop.org/0964-1726/25/7/075025)

IOP Publishing Smart Materials and Structures
Smart Mater. Struct. 25 (2016) 075025 (7pp) doi:10.1088/0964-1726/25/7/075025

Equivalent dynamic model of DEMES rotary joint

Jianwen Zhao[1,2,3], Shu Wang[2], Zhiguang Xing[2], David McCoul[3], Junyang Niu[2], Bo Huang[2], Liwu Liu[1] and Jinsong Leng[1]

[1] Postdoctoral Research Station of Material Science and Engineering, Harbin Institute of Technology, Harbin, 157401, People's Republic of China
[2] Department of Mechanical Engineering, Harbin Institute of Technology, Weihai, 264209, People's Republic of China
[3] Department of Materials Science and Engineering, UCLA, Los Angeles, CA 90095, USA

E-mail: zhaojianwen@hit.edu.cn and wangshuhit14@sina.com

Received 16 July 2015, revised 4 May 2016
Accepted for publication 10 May 2016
Published 10 June 2016

Abstract

The dielectric elastomer minimum energy structure (DEMES) can realize large angular deformations by a small voltage-induced strain of the dielectric elastomer (DE), so it is a suitable candidate to make a rotary joint for a soft robot. Dynamic analysis is necessary for some applications, but the dynamic response of DEMESs is difficult to model because of the complicated morphology and viscoelasticity of the DE film. In this paper, a method composed of theoretical analysis and experimental measurement is presented to model the dynamic response of a DEMES rotary joint under an alternating voltage. Based on measurements of equivalent driving force and damping of the DEMES, the model can be derived. Some experiments were carried out to validate the equivalent dynamic model. The maximum angle error between model and experiment is greater than ten degrees, but it is acceptable to predict angular velocity of the DEMES, therefore, it can be applied in feedforward–feedback compound control.

Keywords: dielectric elastomer, dielectric elastomer minimum energy structure (DEMES), dynamics analysis, artificial muscles, soft robotics

(Some figures may appear in colour only in the online journal)

1. Introduction

Dielectric elastomers (DEs) have been considered to be the best candidate for artificial muscle because of their high-strain response [1–3], high energy densities [4] (seventy times higher than conventional electromagnetic actuators), and high energy conversion efficiencies [5] (60%–90%). Among the different kinds of DE structures, dielectric elastomer minimum energy structures (DEMESs) can realize rotational flexibly. The operational mechanism of DEMES is shown in figure 1, in which unique conformations result from the minimization of the free energy of the DE. After adhering a pre-stretched DE film to a thin elastic frame such as polyethylene terephthalate (PET) [6, 7], acrylonitrile butadiene styrene [8], or polyvinyl chloride [9], the restoring force of the film bends the elastic frame into a minimum energy state. When an adequate electric field is applied across the DE, the frame flattens out and the bending angle decreases. In this way, dynamically changing the voltage can dynamically and continuously alter the joint angle.

To better improve the application of DEMESs to flying and mobile robots, a dynamic model should be established. Thus we can adjust the angular displacement and angular velocity with feedforward control through the model. Typically, the static analysis of DEMESs is partially realized by a free energy function model [11], a combination of the Arruda–Boyce and Neo-Hookean models [12], a hybrid Arruda–Boyce strain energy function augmented with an electrostatic energy density [13], and an extended dynamic relaxation method [14]. The morphology of the DEMES devices is a saddle [9] as shown in figure 2.

The saddle has a complicated stress distribution, so a dynamic model of a DEMES cannot be established by the above methods. In this paper, we will focus on only the

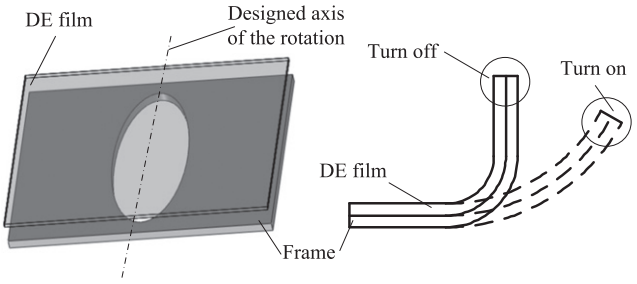

Figure 1. Deformation principle of the DEMES rotary joint [10].

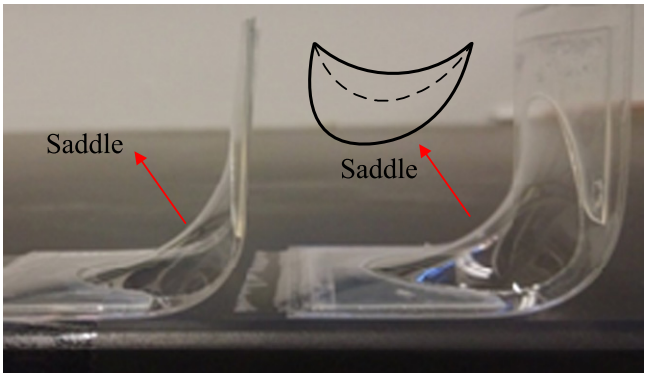

Figure 2. Picture of the DE saddle surface morphology on a DEMES [10].

macroscopic character of the DE film and consider the DE film as a variable stiffness spring. As a result, only two factors will influence the dynamic response: the torque of the DE on the frame and the damping of the DEMES. With this assumption, the complicated stress of the DE film can be avoided and the dynamic response can still be analyzed because of the measurable torque and damping of the DEMES. A method composed of theoretical and experimental results is presented as follows to analyze the dynamic response of DEMESs.

2. Structure and parameters of the DEMES

To restrict frame bending to only one axis, the rigidity of the non-bending edges was enhanced by mounting two stiffening beams as shown in [6] and figure 3, because the DE film is biaxially pre-stretched to ensure sufficient voltage-induced strain.

Let us define the parameters of the structure above as in figure 4; the thicknesses of the primary frame, film, and stiffening frame are greatly exaggerated to show the structure more clearly.

3. Dynamic model of the DEMES

The thickness of the DE film (VHB™ 4910) is 40–50 μm after 400% biaxial prestrain. Since the length after pre-stretching is five times the original length, assuming incompressibility of the DE the calculated final thickness of the DE

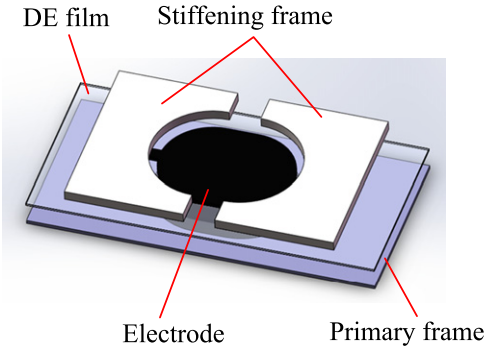

Figure 3. The DEMES rotary joint with semicircular stiffening elements.

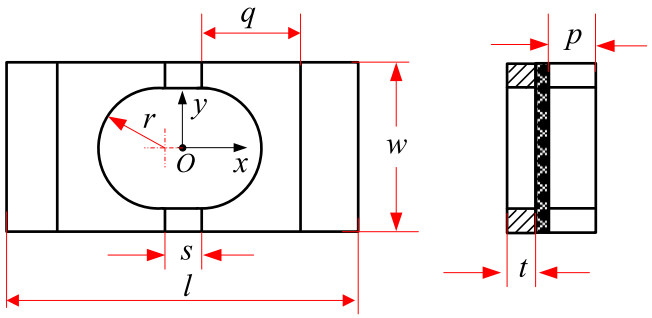

Figure 4. Parameters of the structure. l = total length, w = total width, t = thickness of primary frame (exaggerated), p = thickness of stiffening frame (exaggerated), q = width of each stiffening frame, s = spacing between the stiffening frame, and r = radius of each semicircle [10].

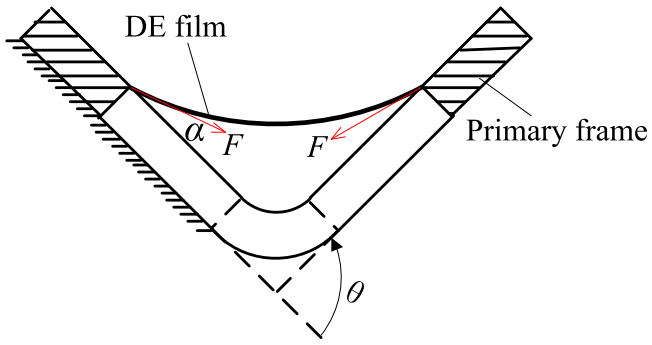

Figure 5. Cross section of the DEMES joint in static equilibrium [10].

film is $1000/25 = 40\,\mu$m. However the true final thickness may be slightly greater than 40 μm, such as 40–50 μm as observed by experiment. The simplified DE film and frame deformation are shown in figure 5. Let θ be the joint bending angle, F be the resultant force of the DE film to the primary frame, and α be the tangent angle between F and the frame. In an idealized case, the deformation of the DEMES would be as shown in figure 5.

Let us treat the active frames (almost half of the primary frame and stiffening frame) as objects and ignore any deformation of the stiffening frame. Then under an applied square wave voltage, the dynamics equation for the active frame can

be written as

$$k_{\mathrm{DE}}(U_{\mathrm{film}},\theta)\theta - k_{\mathrm{f}}\theta - c_{\mathrm{s}}\dot{\theta} - T_{\mathrm{a}} = J_{\mathrm{f}}\ddot{\theta}, \tag{1}$$

where, k_{DE} is the equivalent rotational rigidity of the DE film as a function of voltage and θ, U_{film} is the voltage applied across the DE film, k_{f} is the rotational stiffness of the DEMES rotary joint (which is approximately equal to the rotational stiffness of the primary frame with units of Newton-meters per radian), c_{s} is the damping coefficient of the system (including the damping of the primary frame and the DE film), T_{a} is the resistance torque that the air exerts on the frame, and J_{f} is the rotational inertia of the active frames. Parameters in equation (1) can be calculated as follows

$$k_{\mathrm{f}} = \frac{E(w-2r)t^3}{12s}, \tag{2}$$

$$J_{\mathrm{f}} = \frac{\rho_{\mathrm{f}}}{24}[twl^3 + wp(2q+s)^3 - wps^3 - 2trs^3 - 3\pi r^2(t+p)(r^2+s^2)] \tag{3}$$

and

$$T_{\mathrm{a}} = \frac{1}{2}\int_0^{\frac{l}{2}} C_{\mathrm{d}}\rho_{\mathrm{a}} w(r\dot{\theta})^2 r\mathrm{d}r = \frac{1}{128}C_{\mathrm{d}}\rho_{\mathrm{a}} w l^4\dot{\theta}^2, \tag{4}$$

where E is the Young's modulus of the primary frame and w, r, t, s, l, and p are defined in figure 4. ρ_{f} and ρ_{a} are the density of frame and of air, respectively. C_{d} is the drag coefficient of air on the frame, and for this DEMES $C_{\mathrm{d}} = 1.15$ [15].

In equation (1), k_{DE} is difficult to describe by a theoretical model because the morphology of the DE film is a saddle surface, the stress distribution is quite complicated, and the viscoelasticity of DE film is hard to model. The parameter c_{s} in equation (1) is difficult to model as well, but we can consider the resultant torque of the DE film and frame as the driving torque T_{d}. T_{d} and c_{s} can be measured by experiment, so equation (1) can be calculated.

Furthermore, to calculate equation (1), let

$$T_{\mathrm{d}} = T_{\mathrm{film\_D}}(\theta) + T_{\mathrm{frame}}(\theta), \tag{5}$$

where, T_{d} can be regarded as a driving torque, and $T_{\mathrm{film\_D}}(\theta) = k_{\mathrm{DE}}(U_{\mathrm{film}},\theta)\theta$, $T_{\mathrm{frame}}(\theta) = k_{\mathrm{f}}\theta$. $T_{\mathrm{film\_D}}$ is the torque of DE film to frame during dynamic deformation. Therefore, to calculate equation (1), the parameters c_{s} and T_{d} would need measured, and during this process the relationship between the torques of the DE film during dynamic and static deformations can be analyzed.

4. Measurement of c_{s} and T_{d}

4.1. Measurement of c_{s}

The damping coefficient c_{s} can be calculated by equations (6), (2), (3) and (7) as

$$c_{\mathrm{s}} = \frac{2\sqrt{k_{\mathrm{f}}J_{\mathrm{f}}}}{\sqrt{1+\left(\frac{2\pi}{\ln\eta}\right)^2}}, \tag{6}$$

Table 1. Parameters of the DEMES in experiments (unit: mm).

t	p	q	w	r	s	l
0.17	0.25	30	44	15	8	88

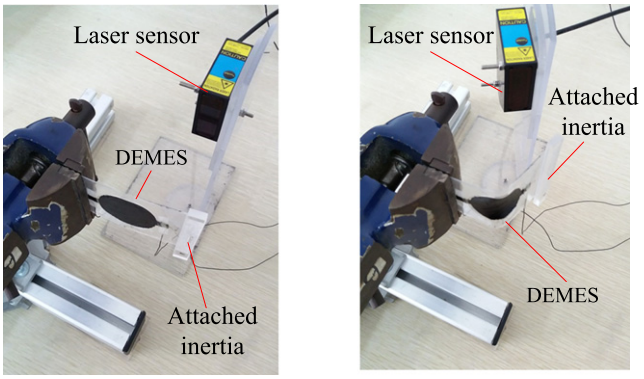

(a) Switch on (b) Switch off

Figure 6. Experiment to measure damping.

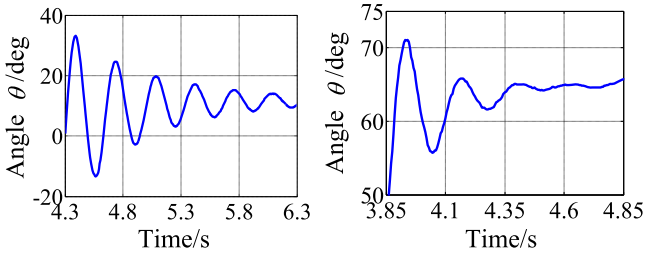

a) Switch on (b) Switch off

Figure 7. Decay curve from experimental measurements.

$$\eta = A_i/A_{i+1}, \tag{7}$$

where, η is a reduction factor, and A_i and A_{i+1} are two neighboring amplitudes on a decay curve of the DEMES during free vibration. This decay curve can be obtained by observation of the DEMES, and parameters of the DEMES are shown in table 1.

A 400% biaxial prestrain is chosen with VHB™ 4910; thus the film can maintain at least 254% prestrain at a 90° initial angle of the DEMES joint [9]. The primary and stiffening frames are made of laser-cut PET with a Young's modulus of 4.25 GPa; more details of fabrication can be seen in [6, 16].

The experimental setup for measuring damping is shown in figure 6, in which an attached inertial mass is mounted to the primary frame while the damping is measured. Both of the attached masses depicted in figures 6(a) and (b) are 3 g.

The decay curve is shown in figure 7.

The damping c_{s} can be calculated by equations (6) and (7), where

$$c_{\mathrm{s}} = \begin{cases} 1.79\times10^{-5}\ \mathrm{N\,s\,m^{-1}} & U_{\mathrm{film}} = 5\ \mathrm{kV}, \\ 4.64\times10^{-5}\ \mathrm{N\,s\,m^{-1}} & U_{\mathrm{film}} = 0. \end{cases}$$

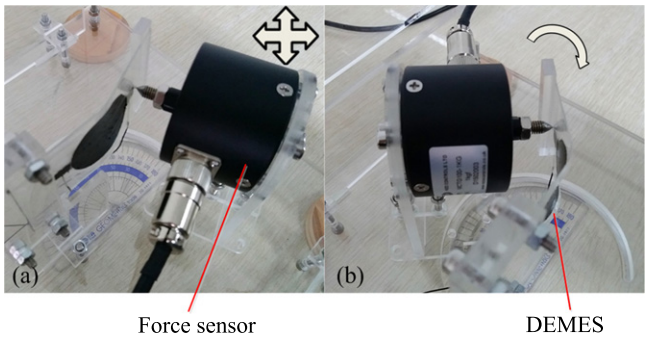

Figure 8. (a) Measurement of T_d while $U_{film} = 0$. (b) Measurement of T_d while $U_{film} = 5$ kV.

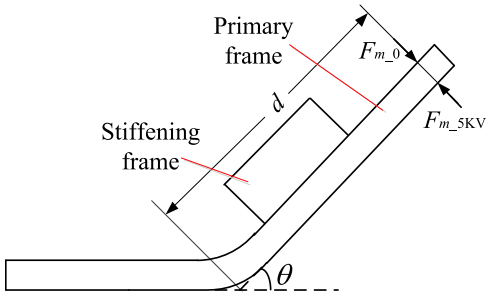

Figure 9. Measurement of T_d. F_{m_0} is the measured value of the force sensor while $U_{film} = 0$, and $F_{m\_5\,kV}$ is the measured value while $U_{film} = 5$ kV.

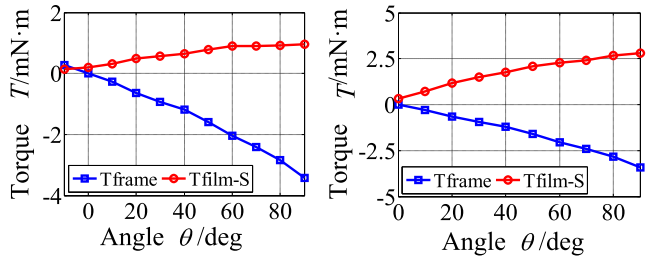

(a) While $U_{film} = 5$ kV (b) While $U_{film} = 0$

Figure 10. The measured torques in experiments.

4.2. Measurement and calculation of T_d

The measurement of T_d in equation (6) was conducted by the system shown in figure 8. The miniature load cells (MCTG100-1 Kg) have three degrees of freedom to ensure the tip is perpendicular to the primary frame and in contact with the same point of the DEMES.

The parameter definitions are shown in figure 9.

Letting counterclockwise rotations be positive and treating the moving part of the DEMES as an object, an equation can be obtained by static equilibrium such that

$$T_{film\_S} + T_{frame} + F_m d = 0, \tag{8}$$

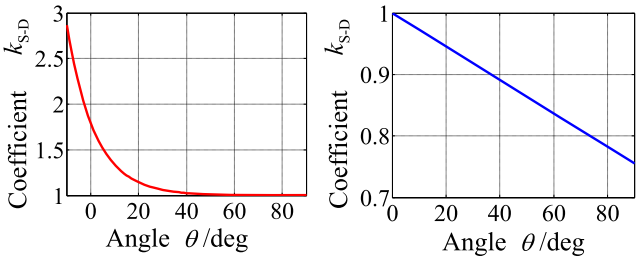

(a) While $U_{film} = 5$ kV (b) While $U_{film} = 0$

Figure 11. The relationship between dynamic and static torque of DE film.

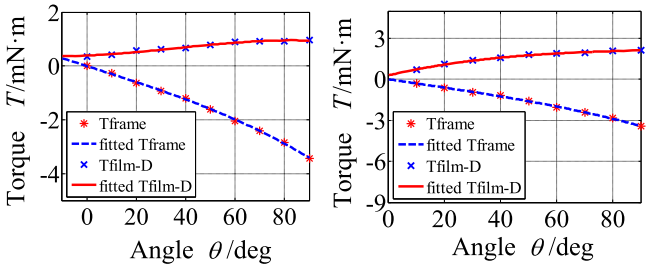

(a) While $U_{film} = 5$ kV (b) While $U_{film} = 0$

Figure 12. The measured and fitted torques in experiments.

where T_{film_S} is the torque of the DE film in the static state. T_{frame} can be measured without the DE film, so T_{film_S} when $U_{film} = 5$ kV and $U_{film} = 0$ can be calculated by equation (8) using the measurement values of $F_{m\_5\,kV}$ and F_{m_0}.

Eleven experimental values were measured for T_{frame} at both $U_{film} = 5$ kV and $U_{film} = 0$, and T_{film_S} at $U_{film} = 5$ kV and $U_{film} = 0$. Their values are plotted in figure 10.

The static torque T_{film_S} is different from the dynamic T_{film_D} because the dynamic conformational entropy is different from the static conformational entropy of macromolecule chains even with same strain of the DE film. The extent of the difference depends on the voltage duration and the deformation angle. If we focus on the DEMES response only under a quick alternating voltage (such as flapping wing [17], then the amount of difference will depend primarily on the deformation angle θ. Let

$$T_{film\_D} = k_{S-D} T_{film\_S}, \tag{9}$$

where k_{S-D} can be obtained by the experimental results as shown in figure 11 where

$$\begin{cases} k_{S-D} = 0.79e^{-0.085\theta} + 1 & U_{film} = 5\text{ kV}, \\ k_{S-D} = -0.0027\theta + 1 & U_{film} = 0, \end{cases} \tag{10}$$

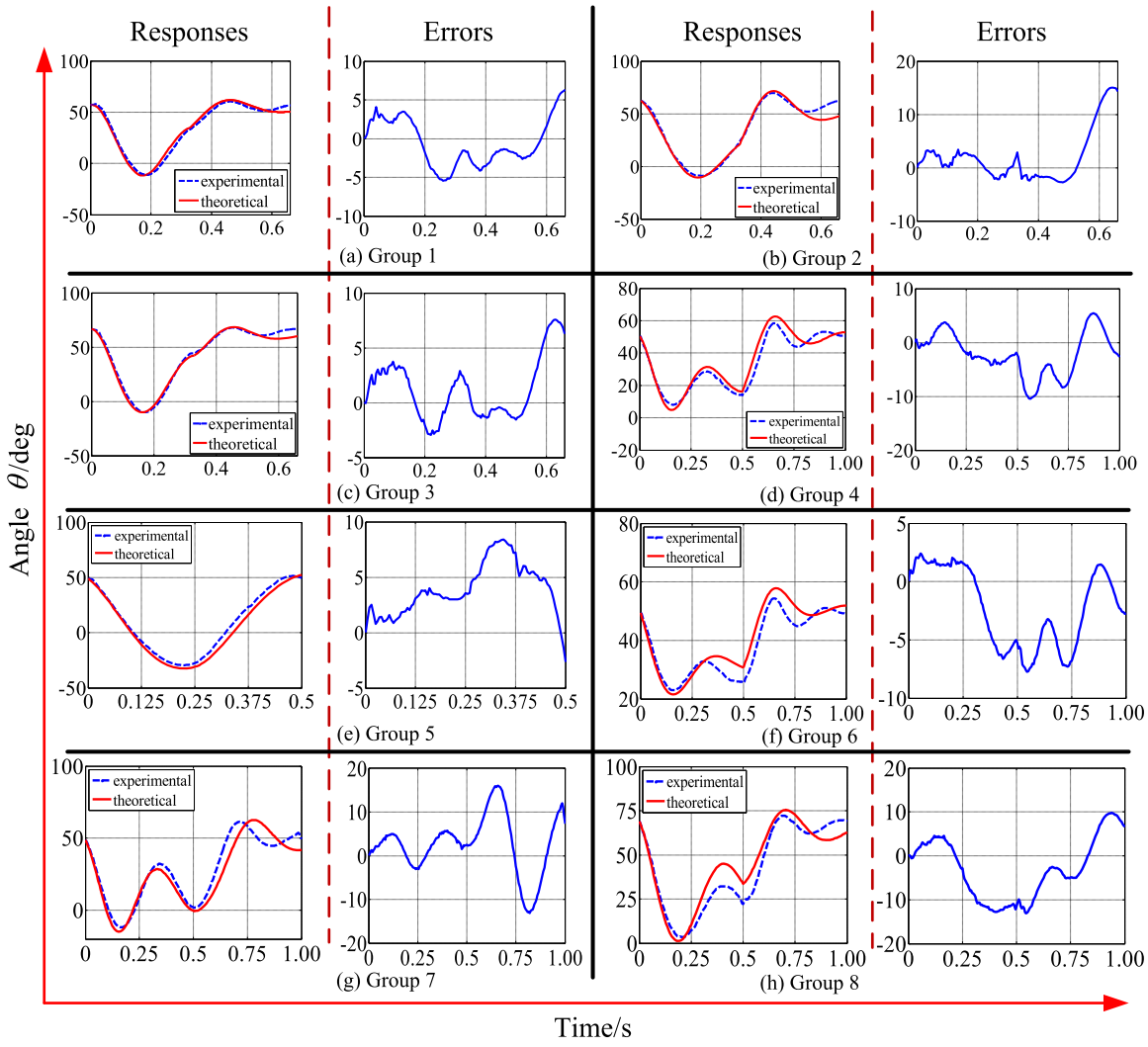

Figure 13. Theoretical and experimental response and error between them with different system parameters.

Table 2. Parameters in the eight groups of experiments.

				Parameters of the DEMES (mm)						
Group number	Voltage (kV)	Frequency (Hz)	Prestrain (% × %)	t	p	q	w	r	s	l
1	5	1.587	400 × 400	0.17	0.25	30	44	15	8	88
2	5	1.587	350 × 350	0.17	0.25	30	42	15	8	88
3	5	1.587	400 × 400	0.17	0.25	30	48	16	8	88
4	5	1	400 × 400	0.19	0.25	29	40	15	8	86
5	5	4	400 × 400	0.19	0.25	29	40	15	8	86
6	4	1	400 × 400	0.19	0.25	29	40	15	8	86
7	5	1	300 × 300	0.19	0.25	28	40	15	10	86
8	5	1	250 × 250	0.19	0.25	27	40	15	13	86

Based on figure 10 and equation (10), the dynamic torque of the DE film $T_{\text{film\_D}}$ can be obtained and fitted as shown in figure 12.

The polynomial function to fit the measured T_{frame} is given by

$$T_{\text{frame}} = -0.2\theta^3 + 0.1\theta^2 + 1.8\theta. \tag{11}$$

The polynomial function to fit the measured $T_{\text{film\_D}}$ is

$$\begin{cases} T_{\text{film\_D}} = -0.26\theta^3 \\ \qquad + 0.48\theta^2 + 0.24\theta + 0.39 \quad U_{\text{film}} = 5\ \text{kV}, \\ T_{\text{film\_D}} = 0.30\theta^3 \\ \qquad - 1.5\theta^2 + 2.7\theta + 0.30 \quad U_{\text{film}} = 0, \end{cases} \tag{12}$$

The polynomial fitting is working only by one function, so it has the advantage of comparison with splined fitting to describe characteristics of the torque.

Based on equations (11), (12) and (5), the driving torque T_d can then be calculated.

5. Comparison between theoretical and experimental results

5.1. Calculation of the dynamic model

Based on above analysis and experimental results, the dynamic model of the DEMES with the parameters in table 1 is

$$\begin{cases} 10^5 T_d - 1.79\dot{\theta} - 2.97 \times 10^{-3}\dot{\theta}^2 = 4.03\ddot{\theta} & U_{film} = 5\ \text{kV}, \\ 10^5 T_d - 4.64\dot{\theta} - 2.97 \times 10^{-3}\dot{\theta}^2 = 4.03\ddot{\theta} & U_{film} = 0, \end{cases} \tag{13}$$

where T_d has already been calculated in section 4.2. Equation (13) contains two nonlinear differential equations for which it is difficult to obtain analytical solutions. In this paper, we numerically solve these equations by the 'ode45' function of MATLAB™ (MathWorks). Comparison of the dynamic response between theoretical calculations and experimental measurements during a voltage cycle are given as follows.

5.2. Comparison of response between theoretical model and experiments

To obtain the response of the DEMES and validate the theoretical model, eight groups of experiments were carried out with different parameters (e.g., dimensions of the DEMES, and the amplitude and frequency of the voltages applied to the DE film). The waveform of voltage is a square wave with duty cycle of 0.5, because the model applies only to a square wave, which is commonly used and allows for the quickest actuation response.

The theoretical and experimental responses, as well as the error between them, are shown in figures 13(a)–(h); the former is shown at left and the latter is shown at right. The system parameters are given in table 2.

5.3. Error analysis

The error can be attributed to several aspects. Firstly, measurement of the driving torque T_d results in a slight error. The error of the force sensor is smaller than 0.1 mN, so the total error of T_d is about 0.005 mN m. The error distribution is symmetrical.

Additionally, the measurement of the damping coefficient c_s results in a slight error as well. The damping coefficient c_s was measured by the laser sensor whose error is smaller than 0.01 mm, that makes slight errors of response measurement with symmetrical distribution. Moreover, the small deformation of the stiffening frame was ignored, that makes the calculation of k_f larger than the real value. Finally, the coefficient k_{S-D} is just a macroscopic and equivalent similarity that maybe brings strong errors.

Actually, the viscoelasticity of VHB™ 4910 is quite high [18], his static viscoelastic creep can be eliminated by pre-programmed voltage, but dynamic viscoelastic performance is pretty complicated, therefore, dynamic response is difficult to be modeled precisely.

To sum up, the error of deformation angle is not negligible, but it is acceptable to velocity prediction of feedforward–feedback compound control for a flapping wing, because the error can be compensated by the feedback controller.

6. Conclusion

The dynamic model of the DEMES is difficult to be constructed because of the complicated morphology and viscoelasticity of the DE film. In this paper, composing theoretical analysis and experimental measurement, an equivalent dynamic model of a DEMES rotary joint was established. Computation of the model depends upon the measurements of driving torque and of the damping coefficient. The error of angular displacement is not small, but it is acceptable to feedforward–feedback compound control, such as for flapping wings or other devices actuated by the DEMES rotary joint.

This model ignores the internal stress of the DE film and simply focuses on the macroscopic characteristics. As a result, this model is not a pure dynamic model, but rather can be applied to feedforward control of the DEMES, as well as to design other similar complicated structures.

In addition, this method composed of theoretical analysis and experimental measurement can be applied to model complicated dynamic responses in similar systems.

References

[1] Pelrine R *et al* 2000 High-speed electrically actuated elastomers with strain greater than 100% *Science* **287** 836–9
[2] Brochu P and Pei Q 2010 Advances in dielectric elastomers for actuators and artificial muscles *Macromodecular Rapid Commun.* **31** 10–36
[3] Zhao X and Suo Z 2010 Theory of dielectric elastomers capable of giant deformation of actuation *Phys. Rev. Lett.* **104** 178302
[4] Wingert A, Lichter M D and Dubowsky S 2006 on the design of large degree-of-freedom digital mechatronic devices based on bistable dielectric elastomer actuators *IEEE/ASME Trans. Mechatronics* **11** 448–56
[5] Karpelson M, Wei G-Y and Wood R J 2008 A review of actuation and power electronics options for flapping-wing robotic insects *IEEE Int. Conf. on Robotics and Automation* pp 779–87
[6] Kofod G, Paajanen M and Bauer S 2006 Self-organized minimum-energy structures for dielectric elastomer actuators *Appl. Phys.* A **85** 141–3
[7] David M C and Qibing P 2015 Tubular dielectric elastomer actuator foractive fluidic control *Smart Mater. Struct.* **24** 105016

[8] Petralia M T and Wood R J 2010 Fabrication and analysis of dielectric-elastomer minimum-energy structures for highly-deformable soft robotic systems *2010 IEEE/RSJ Int. Conf. on. Intelligent Robots and Systems (IROS)* (Piscataway, NJ: IEEE) pp 2357–63

[9] Buchberger G *et al* 2014 Temporal change in the electromechanical properties of dielectric elastomer minimum energy structures *J. Appl. Phys.* **115** 214105

[10] Zhao J *et al* 2015 Improvement on output torque of dielectric elastomer minimum energy structures *Appl. Phys. Lett.* **107** 063505

[11] Zhao X and Suo Z 2008 Method to analyze programmable deformation of dielectric elastomer layers *Appl. Phys. Lett.* **93** 251902

[12] O'Brien B *et al* 2008 An experimentally validated model of a dielectric elastomer bending actuator *The 15th Int. Symp. on: Smart Structures and Materials & Nondestructive Evaluation and Health Monitoring* (International Society for Optics and Photonics) pp 69270T–11

[13] O'Brien B, Gisby T, Calius E, Xie S and Anderson I 2009 FEA of dielectric elastomer minimum energy structures as a tool for biomimetic design *Proc. SPIE* **7287** 728706

[14] Siu S *et al* 2013 Dynamic relaxation study and experimental verification of dielectric-elastomer minimum-energy structures *Appl. Phys. Lett.* **103** 171906

[15] Chen F, Quan X and Song Y 2015 *Fundamentals of Aerodynamics* 1st edn (Harbin, China: Harbin Institute of Technology Press) pp 49–120

[16] Lai W *et al* 2012 Fabrication and analysis of planar dielectric elastomer actuators capable of complex 3D deformation *IEEE Int. Conf. on Robotics and Automation (ICRA)* pp 4968–73

[17] Zhao J, Niu J, McCoul D, Leng J and Pei Q 2015 A rotary joint for a flapping wing actuated by dielectric elastomers: design and experiment *Meccanica* **50** 2815–24

[18] Zhang J, Wang Y, McCoul D, Pei Q and Chen H 2014 Viscoelastic creep elimination in dielectric elastomer actuation by preprogrammed voltage *Appl. Phys. Lett.* **105** 212904